Functionalization of Magnetic Nanoparticles with Deoxynucleotide Triphosphates for Utilization in DNA Sequencing

A THESIS SUBMITTED TO THE

FACULTY OF THE UNIVERSITY OF

MINNESOTA BY

Calvin Nazareth

IN PARTIAL FULFILLMENT OF THE

REQUIREMENTS FOR THE DEGREE OF

MASTER OF SCIENCE

Advisor: **Kevin D. Dorfman**

February 2023

Acknowledgements

I would like to begin by expressing my gratitude to the people at Seagate who enabled me to complete this project. Firstly, I thank my managers and director who gave me permission to work on this project while working for their teams. So, thank you to Rick Shurts, Chuck Hawkinson, and Jim Price. Next, I thank Gemma Mendonsa, Anil Reddy, and James Froberg who are part of the Seagate Research Group running this project. Their expertise and input was invaluable to my progress in this project. Thank you also to Xiaoxiao Yao and Peng Ge, two interns who worked in the lab with me. Finally, I express my gratitude to the numerous Seagate employees who helped me with characterization and will be listed by name in the Statement of Contributions.

I am also grateful to the people at the University of Minnesota who were instrumental in my progress through this project. I thank Aditya Bhan who was the DGS when I began my program. Thank you also to Julie Prince who has dealt with my numerous logistical questions and aided me in getting everything set up so that I can graduate. I appreciate all the professors and TAs who taught my courses and helped me as I worked through my degree. Most importantly at the university, a huge thank you to Prof. Kevin Dorfman for agreeing to be my advisor and guiding me through this unconventional degree program and research project.

Last, but not least, I need to thank all the people in my life who were not directly part of my project or degree progression. The most gratitude goes to my parents, Martin and Sarita Nazareth, who raised me and were my first teachers. They instilled in me a love for learning and the drive for academic excellence. I thank my brother and sister, Andrew and Tricia Nazareth, who have put up with me for the majority of their lives. I am so lucky to have such a loving family. Lastly, I thank all my friends and family in the Twin Cities who have been there for me even as I ignored them to spend time working on this project.

Dedication

Because none of my family members
told me what they want for Christmas, I
am dedicating this thesis to them,
my mom, dad, brother, and sister,
and will consider that their Christmas present.

Abstract

Current methods for DNA sequencing leave a lot to be desired. There is immense research focused on developing methods to sequence longer and larger samples of DNA and to do so more rapidly. One possible new approach to DNA sequencing uses magnetically labeled deoxynucleotide triphosphates (dNTPs) as the complimentary bases for a sequencing-by-synthesis approach. The polymerase in this system would be immobilized on a sensor so that when the nucleotide is attached to the growing strand, the sensor can detect the signal. As the polymerase completes the strand for DNA extension, the signal from each magnetic nanoparticle (MNP) is recognized and generates a sequence.

The contents of this thesis provide results for two critical initial steps in developing the proposed method. Firstly, we attached dNTPs to magnetic nanoparticles to create dNTP-MNP conjugates. We attempted two methods of conjugation with numerous characterization techniques to confirm the attachment. Secondly, we studied how the dNTP-MNP conjugation affected the dNTPs in quantitative polymerase chain reaction (qPCR) to model how they would interact with a polymerase in a hypothetical sequencer. The characterization results confirmed the conjugation of the dNTP to the MNP. qPCR was performed with various conditions and solvents which led to the conclusion that the MNP conjugation does not hinder polymerase interaction with the dNTP. This is a crucial result for the development of such a sequencer by providing the groundwork for the continuation of the project.

Table of Contents

List of Tables and Figures

List of Abbreviations

DNA – Deoxyribonucleic Acid

mRNA – messenger Ribonucleic Acid

NGS – Next Generation Sequencing

HGP – Human Genome Project

PCR – Polymerase Chain Reaction

dNTP – Deoxynucleotide Triphosphate

MNP – Magnetic Nanoparticle

dNTP- MNP – system of dNTPs conjugated to an MNP

EDC – 1-Ethyl-3-(3-dimethylaminopropyl)carbodiimide

PEG – Polyethylene glycol

HPLC – High-performance Liquid Chromatography

MS – Mass Spectrometry

FTIR – Fourier Transform Infrared Spectroscopy

XPS – X-ray Photoelectron Spectroscopy

SEM – Scanning Electron Microscopy

TEM – Transmitting Electron Microscopy

STEM – Scanning TEM

EDS – Energy Dispersive X-ray Spectroscopy

qPCR – quantitative PCR

Statement of Contributions

The research and design of this project was generated by Gemma Mendonsa and Anil Reddy at Seagate Research Group. The PEG conjugation method was initially proposed by Gemma Mendonsa, and the EDC method was proposed by Xiaoxiao Yao. All experiments and trials for MNP conjugation and PCR for the project were completed by Calvin Nazareth, and Calvin wrote all the material in the thesis.

All the characterization techniques were completed with Seagate instruments and in some cases by specialists at Seagate. All samples were prepared by Calvin Nazareth except TEM. HPLC-MS for the PEG intermediates was run by Summer Chen. Summer Chen and Xiaoxiao Yao ran the FTIR samples. Calvin acquired all XPS data, with training on the instrument from Vivien Talghader. SEM samples were imaged by David Keller. TEM samples were prepared and imaged by Karl Foster and Stephen Exarhos with assistance from Carol Johnson. All data were analyzed by Calvin, often with help from a specialist in the characterization technique.

For qPCR, all experiments were run by Calvin Nazareth. Gemma Mendonsa was instrumental in training and developing the qPCR protocols that were used. Gemma was also extremely helpful in the making and running of the gel for gel electrophoresis.

Chapter 1: Introduction

Possibly the most influential discovery in the realm of DNA research came in 1953 when the double helical structure of DNA was discovered [1]. Since then, DNA has been a focus of a wide range of research. DNA is a natural biopolymer that encodes the genetic makeup of humans and animals. Each of the two strands in the double helix is composed of a deoxyribose sugar ring and phosphate backbone as depicted by Watson and Crick and shown in Figure 1.1. The two strands are connected by the nitrogenous bases adenine (A), cytosine (C), guanine (G), and thymine (T).

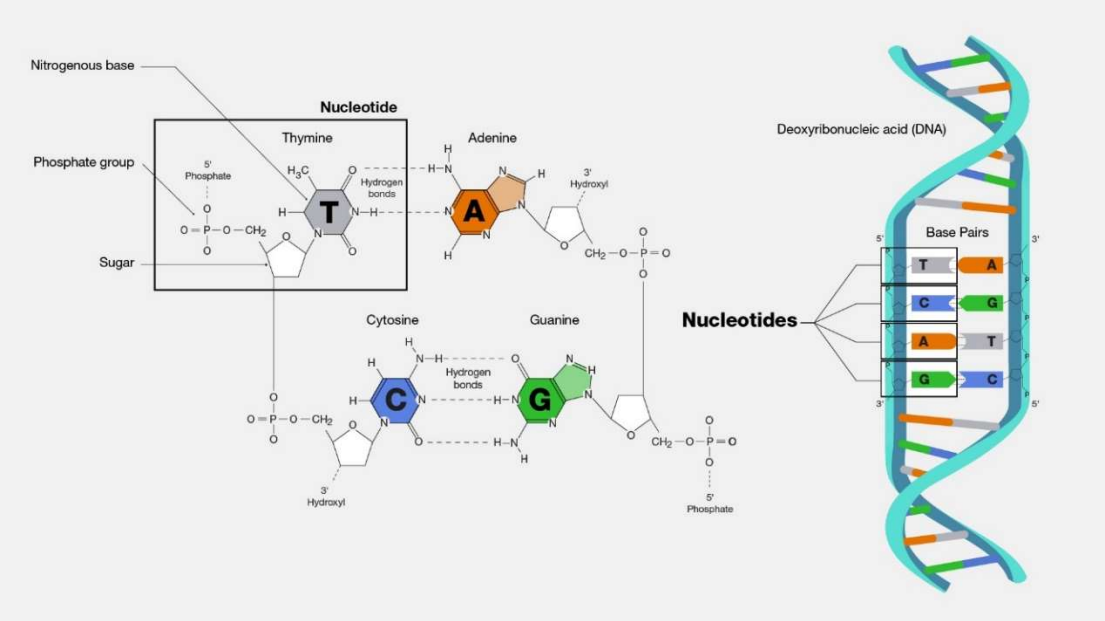

Figure 1.1: Diagram of nucleic acids assembly into DNA double helix structure. Reproduced from Ref. [2].

Nucleic acids represent a quickly growing field with vast possibilities. Vaccinations using mRNA technology are at the forefront of medical innovation. DNA also has myriad possibilities including DNA-based data storage with DNA computing [3]. Genomic sequencing projects in particular have been increasing rapidly in the past

few years at a rate greater than Moore's Law [4,5]. Forensic scientists can use DNA sequencing to identify individuals based on DNA traces [6]. Another group has used sequencing with barcodes to map neuronal connections [7]. Nucleic acid experimentation and DNA sequencing provides a landscape for many possibilities and improvements.

Genomic sequencing is intriguing because it enables greater understanding of humanity and evolution as well as endless possibilities in medicine. It can also be useful outside of biological applications for systems like data storage [3]. Prior to DNA sequencing, protein sequencing and RNA sequencing was explored and developed in the 1950s [8]. They both used similar methods of fragmentation, followed by separation with chromatography and electrophoresis, and then sequence determination by overlapping sequences [9]. The first sequencing technologies for DNA were developed in the early 1970s using chromatography, with Wu sequencing 12 bases of bacteriophage lambda and Gilbert and Maxam sequencing 24 bases of the lactose repressor binding site [10,11].

Sanger sequencing emerged around 1976. It utilized polymerase to extend labelled DNA primers with chain-terminating nucleotides to produce DNA fragments of different lengths [12]. The fragments were analyzed using electrophoresis on polyacrylamide gels with one lane per base. The gels were imaged with x-ray film to produce a ladder image and generate a sequence [13]. This exponentially increased sequencing lengths and speeds. By 1987 there were numerous automated Sanger sequencing machines able to sequence thousands of bases each day [14,15]. The Sanger

sequencing technique then became the common method for sequencing and was the primary technique used in the Human Genome Project (HGP) [16].

In the late 1990s and early 2000s, Sanger sequencing was superseded by Next Generation Sequencing (NGS). The first commercial NGS instrument was released in 2005 from 454 [8]. Like 454 Sequencing, most NGS strategies use PCR to amplify DNA samples coupled with fluorophore labels to identify individual nucleotides [17]. Other developing sequencing techniques include optically mapping synthesis in real time and measuring fluorescence of incorporated nucleotides [18,19]. Some of the top-level sequencers available include the NovaSeqX Plus from Illumina which they report 16 Tb yield and uses NGS [20]. The Revio from PacBio uses optical sequencing and reports 90 Gb yield with 99.95% read accuracy [21]. For comparison, the HGP draft human genome had ~23 Gb generated.

Our group has proposed a novel method for DNA sequencing using magnetically labelled deoxynucleotide triphosphates (dNTPs) as an adaptation of sequencing-by-synthesis. Figure 1.2 depicts the sequencing mechanism. Each type of dNTP will be attached by its γ phosphate to a unique size of magnetic nanoparticle (MNP). Polymerase will be immobilized on the surface of a sensor, and the dNTP-MNP conjugates will flow over the polymerase sensor apparatus. As the polymerase completes the DNA amplification, the sensor will sequentially detect the MNP from which each nucleotide is being cleaved thus generating a sequence.

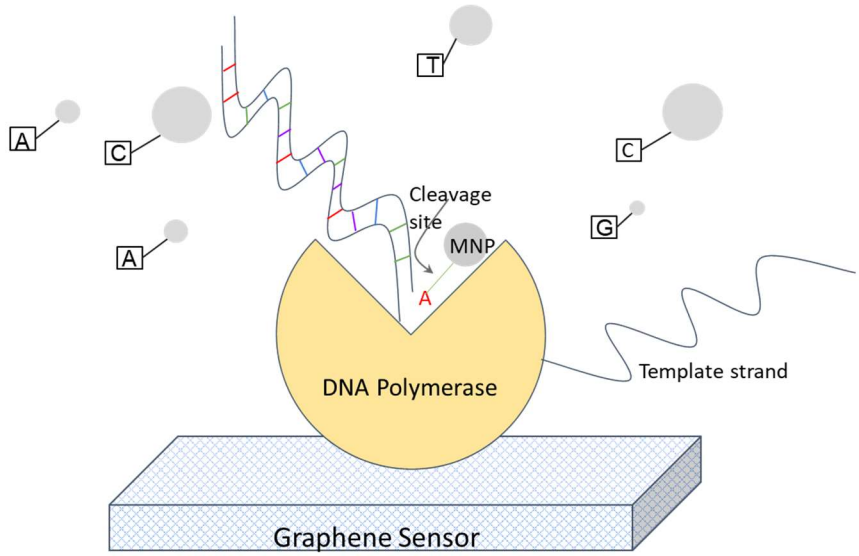

Figure 1.2: Schematic for proposed sequencing apparatus. Polymerase attaches complimentary nucleotides to the template strand by cleaving from the MNP. The sensor detects the MNP from which the nucleotide is cleaved.

Like Illumina, our proposed method also uses PCR, however, the dNTPs are labeled with MNPs on the γ phosphate rather than fluorophores. MNPs are advantageous because composition of magnetic material does not degrade the way fluorophores degrade. MNPs also present a higher signal-to-noise ratio than fluorophores which theoretically would provide an improved detection accuracy for each base as well as increased read length overall. Here, we discuss progress on two essential steps for success of this project: First, we outline the reaction of attaching dNTPs to MNPs. Second, we demonstrate how dNTP-MNP conjugates interact with polymerase.

Chapter 2: Nanoparticle Conjugation

2.1 Introduction

Our proposed sequencing method involves magnetically labeling nucleotides, and subsequently reacted them with polymerase to amplify template DNA with the labeled nucleotides. In polymerase chain reactions (PCR), dNTPs of all four bases are added to reaction mix solution. When adding each nucleotide to the chain, polymerase cleaves off the β and γ phosphates. The following conjugation methods attach the dNTP to the MNP at the γ phosphate. Therefore, as the polymerase attaches the complimentary base to the primer extension, that base will be cleaved from the MNP. The sensor should be able to sense the nanoparticle as the polymerase cleaves the nucleotides.

The first conjugation approach uses direct conjugation to the nanoparticle. Using EDC as a coupling agent, the γ phosphate of the dNTP is attached to amine groups in the coating of a purchased nanoparticle (Figure 2.1) [22]. The only separation between the dNTP and MNP are the polymer coating that came with the purchased MNP and the phosphate chain on the dNTP. With that approach, there is a possibility of steric hindrance where the nucleotide will be too close to the nanoparticle so that the polymerase cannot cleave at the α phosphate (Figure 2.1).

To account for possible steric hindrance, a second method was attempted as well. This method uses a polyethylene glycol (PEG) linker to create a longer link between the nucleotide and MNP [23]. Using the linker, the dNTP will have more clearance from the MNP and should be able to freely interact with the polymerase.

However, this approach could produce issues with signal from the MNP if the PEG chain is too long.

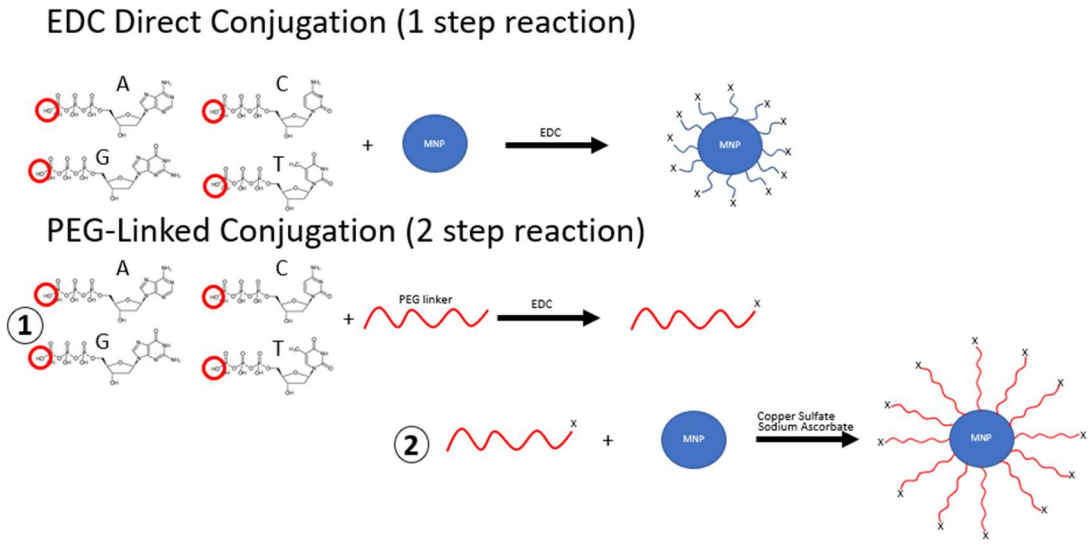

Figure 2.1: Reaction scheme for dNTP-MNP conjugation. **(A)** EDC direct conjugation with dNTPs reacting with MNP using EDC as a coupling agent. **(B)** PEG-Linked conjugation has dNTPs coupled to PEG linker using EDC and dNTP-PEG attaching onto MNP using Cu catalyzed click chemistry.

2.2 Methods & Materials

2.2.1 Conjugation

The first method is a single step reaction using 1-Ethyl-3-(3-dimethylaminopropyl)carbodiimide (EDC) (SigmaAldrich) as a coupling agent to attach the γ phosphate of a dNTP to a magnetic nanoparticle (MNP) (Figure 2.1). PCR grade dNTPs were purchased from ThermoFisher. MNPs were purchased with functional group coatings (OceanNanotech, SigmaAldrich). Both carboxyl and amine terminated MNPs have been experimented with to attach with the γ phosphate of the nucleotide.

The second method uses a two-step reaction to attach the dNTP to the nanoparticle. This protocol is derived from Serdjukow et al. synthesis of gamma-labelled nucleoside triphosphates [23]. The first step involves EDC as a coupling agent to attach a polyethylene glycol (PEG) to the γ phosphate of a dNTP. The PEG linker is purchased with an amine functional group on the terminal that will react with the dNTP and an alkyne functional group on the free terminal (SigmaAldrich). The second step of the reaction is a standard copper-catalyzed click chemistry reaction attaching the alkyne end of the PEG chain to an azide functional group on purchased nanoparticles [23]. The copper added for catalysis is Cu(II) in the form of copper sulfate (Millipore Sigma). Sodium ascorbate is used to reduce to Cu(I).

To purify the dNTP-MNP conjugates, samples were mixed with 300 μl of DI water to completely suspend the solution. The samples were then centrifuged at 10000 rpm for 12 minutes to concentrate the MNPs at the bottom of the tube. The supernatant

was removed. The suspension, centrifugation and supernatant removal was done three times. Samples were stored in aqueous solution.

2.2.2 Characterization

2.2.2.1 HPLC – MS

High-performance liquid chromatography (HPLC) combined with mass spectrometry (MS) is a very common method for chemical analysis. HPLC uses a packed column to separate chemical compounds based on characteristics such as size or polarity. The given sample is divided into fractions based on the time taken to elute from the column. Those fractions are then analyzed using MS to determine the molecular weight of the compound in each fraction. The fractioning by the HPLC isolates the different chemicals in the sample, which purifies the desired product in its fraction.

HPLC was used only on the product of the first step of the PEG two-step reaction process to confirm attachment of the dNTP and PEG chain. The HPLC-MS process was run on UltiMate HPLC 3000 for HPLC with negative mode using acetonitrile and DEA (20 mM DEA in DI water) mobile phases. The flow rate was 0.5 ml/min with a 2.5 µl injection volume. Sample ran through an Acclaim rslc120 C18 reverse-phase (2.2 µm 120 Å 3.0x100 mm) column at 40 °C for 28 minutes. The column specifications include 2.2 µm particle size, 120 Å average pore diameter, and 3.0x100 mm column length (ThermoFisher). HPLC fractions were analyzed with mass spectrometry (MS) to determine the mass of the compounds in each fraction and determine whether the desired product was present. Other reaction products were not

used with this technique because the MNPs would have caused issues with both HPLC and MS. MS was run on ThermoFisher Exactive Plus Mass Spectrometer.

2.2.2.2 FTIR

Fourier transform infrared spectroscopy (FTIR) was used to determine whether nucleotides were attached to nanoparticles by identifying bond signals. FTIR submits a sample to an infrared radiation source. Different bonds absorb energy at different wavelengths. The instrument detects the wavelengths of light that are absorbed by and transmitted through the sample. These signals are Fourier transformed to develop the spectra as a function of the wavenumber. Samples were prepared by suspension in ethanol. They were pipetted and dropped onto the instrument sample holder and solvent was allowed to evaporate before measurement. Measurements were taken with Nicolet iS50 FTIR from ThermoFisher.

2.2.2.3 XPS

Another technique used to characterize the dNTP-MNP conjugation was X-ray photoelectron spectroscopy (XPS). XPS is a surface characterization method that uses an X-ray beam to excite and emit electrons from sample materials. It detects the energies of the emitted electrons and can use the incident X-ray energy to determine binding energy on the surface of the material. Based on the binding energy it can determine elemental composition as well as chemical states. XPS can also determine binding environments and has other functions as well.

XPS samples were prepared from the aqueous synthesis products. The solvent was evaporated from the MNP-dNTP conjugates in water leaving a powder form. The

dNTP-MNP powder was immobilized on carbon tape on a VPIII 60mm platen sample holder. Scans were run on PHI VersaProbe III Photoelectron Spectrometer with x-ray set to 200u25W15KV. Those X-ray settings produce a 200 μm diameter generated by 25 W power and 15kV voltage. The scans included a survey scan from 0 to 1200 eV with a pass energy of 224 eV and focused scans for phosphorus from 123 to 143 eV and pass energy of 55 eV all at 50 ms per step. Each cycle had 1 sweep of the survey and 5 sweeps of the phosphorus scan with 5 cycles per run.

2.2.2.4 Electron Microscopy

Electron microscopy is an imaging technique that subjects a sample to an electron beam and detects the electrons after they interact with the sample to create an image. Scanning electron microscopy (SEM) utilizes secondary scattered electrons to form an image. Transmitting electron microscopy (TEM) has a stronger beam that penetrates the sample. TEM uses electrons from the direct beam and transmitted scattered electrons to generate an image. SEM samples were prepared from the aqueous synthesis products. The solvent was evaporated from the MNP-dNTP conjugates in water leaving a powder form. The powder was immobilized on carbon tape that was placed on a metal holder. Images were taken using Hitachi Regulus 8230 High Resolution Scanning Electron Microscope.

For TEM, samples were prepared using the drop-casting method using 300 μm lacey carbon-coated copper mesh grids (Ted Pella). Samples were diluted in water, a small droplet of the diluted and dispersed sample was dropped onto a clean TEM grid surface, and the solvent was allowed to evaporate. TEM images were acquired with a ThermoFisher Talos F200 G2 with 200 kV accelerating voltage and a ThermoFisher

Ceta 16M CCD. Bright field TEM was selected for survey imaging of the samples to limit beam damage to the organic ligands, and a 70 μm objective aperture was used to further reduce beam damage and to improve image contrast. Minimal sample damage was observed during survey imaging. Scanning TEM mode (STEM) was used to acquire composition maps using Energy Dispersive X-Ray Spectroscopy (EDS) with a ThermoFisher Super-X EDS Detector with a 150 μm condenser-2 aperture inserted. Maps were acquired over regions of interest with 50 μs dwell time and 25 frames with drift correction. EDS maps were processed using recommended pre- and post-filtering in ThermoFisher Velox software.

2.3 Results & Discussion

2.3.1 HPLC

Ideally, all products could be analyzed using LC-MS. That would enable determination of chain length on the MNP and the extent of reactions. However, the this was not possible. For LC, it would be difficult to design a column that would effectively fractionate the samples. Reacted and unreacted MNPs would have overlapping elution peaks due to the dNTP size being ~1 nm compared to MNPs being >30 nm with a wide size distribution. Some sort of affinity chromatography could be possible, but the difference in size of the dNTP and MNPs could still cause issues. Also, the unknown polymer coating from the MNP manufacturers could skew the results. Further, the MNPs were all 30 nm or larger, and with the possibility of the magnets aggregating, it would be risky to add those to either HPLC or MS injection systems.

The only experimental product that could successfully be run through HPLC-MS was the product of the first reaction of the PEG-alkyne method. As it was not attached to an MNP and was just dNTP+PEG. For all four dNTP types, HPLC-MS confirmed conjugation of PEG to dNTP (Figures A.1 and A.2). HPLC would also be ideal for purifying the desired samples. However, since the MNPs were unable to be run through the columns, the samples were purified using centrifugation combined with rudimentary magnetic separation.

2.3.2 FTIR

To characterize the dNTP-MNP conjugates, FTIR was attempted. FTIR has been effective in analyzing nanoparticles and nanoparticle conjugation [24,25]. The key signal that was being investigated was the P-O bond in the phosphates at the end

of the dNTPs. If the MNP samples have phosphate, then that would confirm conjugation of the dNTP to the MNP. The P-O bond signal should show up around between 1300 and 1195 cm^{-1} [26]. C-N and C-O bonds also appear in that range [26]. Figure 2.2 shows that both the EDC and PEG samples had peaks in that region. But since there are so many peaks in that range, the C-N peaks could not be differentiated from the P-O peaks.

The MNPs used for the PEG method had azide terminals, and azide signal appears around 2100 cm^{-1} [27]. However, there is a wide CO_2 background peak in the same region that when subtracted from the spectra, also removes the azide peak. We were unable to isolate the azide peak from the CO_2 peak to confirm azide signal from the unreacted MNP and no azide signal in the reacted MNP. Figure 2.2A shows the unsubtracted CO_2 peak that may include an azide peak as well. Still, some peaks were labelled showing many of the bonds that are present in dNTPs.

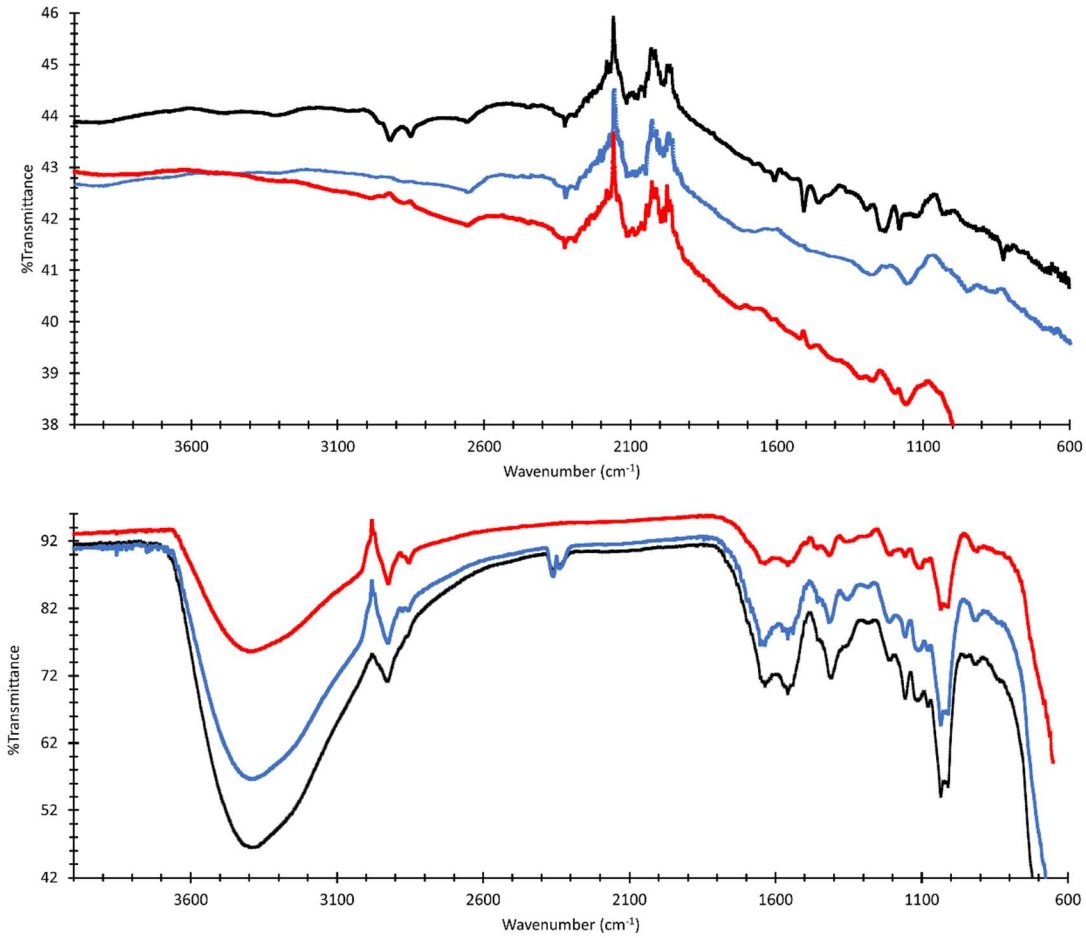

Figure 2.2: FTIR scans of %Transmittance as a function of wavenumber. **(A)** PEG samples - unreacted azide MNPs, dNTP-MNP1, dNTP-MNP2 - from top to bottom. Both experimental samples are replicates. **(B)** EDC samples – dNTP-MNP1, dNTP-MNP2, control unreacted MNP - from top to bottom. Both experimental samples are replicates.

2.3.3 XPS

XPS was utilized to analyze surface composition and determine the presence of phosphorus. The unreacted MNPs should not have any phosphorus in their elemental composition, but the dNTPs have a triphosphate group. Receiving a phosphorus signal from dNTP-MNP conjugates but with no signal from unreacted MNPs could confirm presence of dNTPs on the MNP surface. The data for both reaction methods show

dNTP conjugation to MNP. Figure 2.3B shows the sample signals for dNTP-MNPs vs unreacted MNP control. The dNTP reacted MNPs showed signal at ~133 eV, which signals the presence of phosphorus, whereas the controls show no signal in that range.

Although XPS confirmed the presence of dNTPs in the MNP sample, it was a qualitative result. We were unable to quantify the reaction yield from this analytic technique. In sample prep, the sample in powder form was deposited on carbon tape. The sample thickness was not necessarily uniform across the tape so taking a reading at one point on the sample would yield different results than taking a reading at another point on the sample. Further, there could be alignment issues where choosing a point in the software may be slightly off from that point on the actual sample. These issues made it challenging to quantify the result.

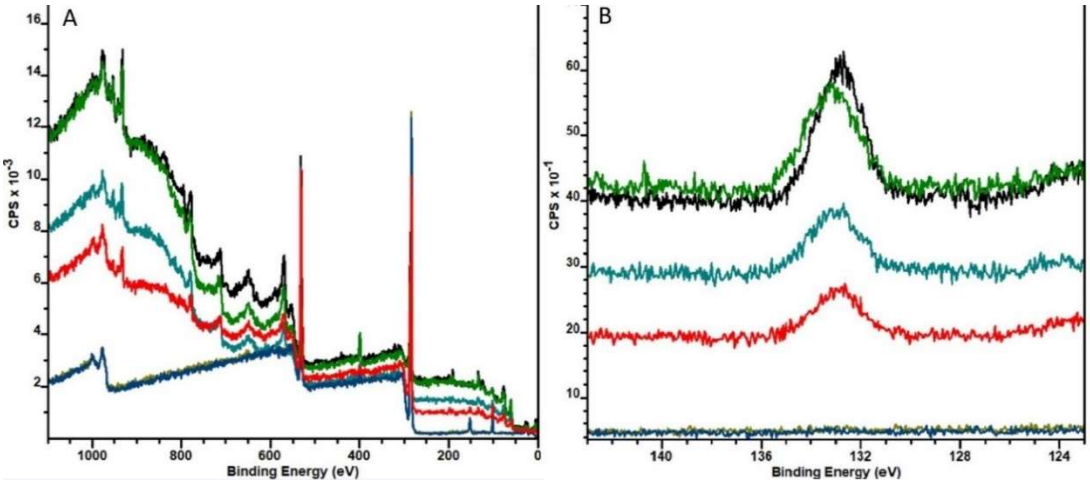

Figure 2.3: XPS results plotted as Counts per Second (CPS) vs Binding Energy. **(A)** Survey scan with broad range of binding energy. **(B)** Focused scan at 133eV – the binding energy for phosphorus (P2p) – showing phosphorus in experimental samples (4 traces with peaks) and no signal from controls (2 flat traces at the bottom).

2.3.4 Fluorescence

Fluorescence was attempted to quantify the conjugation results. The process was first attempted for the PEG samples and included reacting a fluorophore with unreacted MNP to determine a baseline of fluorescence for the MNPs. Then the dNTP-MNP conjugates would be reacted with fluorophore and measured. The difference in the fluorescence, in principle, could be used to determine an approximate reaction yield for the dNTP-MNP conjugation. Cy5 and Cy7 were purchased with alkyne terminals were reacted with the azide MNPs via copper catalyzed click chemistry. Neither fluorophore fluoresced in the established wavelength range, and the peak heights were not constant. These issues could be due to error in the instrument, the experiment, or the reagents. Establishing a baseline fluorescence did not work out, and this technique was not pursued further.

2.3.5 Electron Microscopy

Electron microscopy was used as an attempt to determine the radius of the unreacted MNPs and show an increase in radius for the dNTP-MNP conjugates. SEM was attempted first to visualize the polymer coating on MNPs. The goal was to determine an approximate radius for unreacted MNPs and for dNTP-MNP conjugates and calculate the difference to determine approximate dNTP concentration on the surface. The only MNPs used with this method were azide Turbobeads. The images showed that the radii of the MNPs were not uniform and these MNPs would not be useful for this project moving forward (Figure 2.4). It was also difficult to isolate the dNTPs from the polymer coating of the MNPs as they are both hydrocarbon dominant.

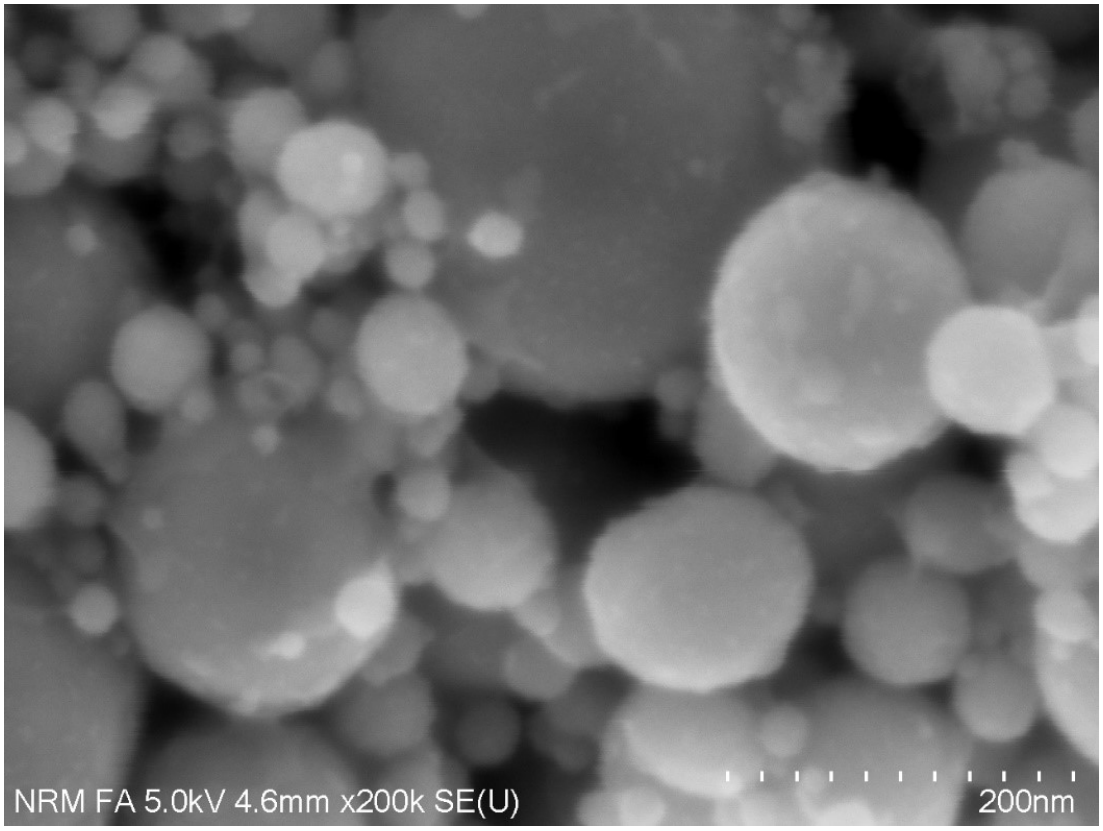

Figure 2.4: SEM image of azide turbobeads. It shows nonuniformity of particle size for initial MNPs.

TEM was attempted after SEM. TEM uses a stronger electron beam and detects electrons that transmit through the sample so it can get better resolution at smaller field of view (FOV). The images taken with TEM were of the azide nanoparticles (OceanNanotech) and carboxyl nanoparticles (OceanNanotech). Both showed good size uniformity. The azide MNPs look like they are single chunks of magnetic metal covered in a polymer coating (Figure 2.5A and B). The carboxyl MNPs are tiny (<10 nm) magnetic particles held together in a polymer matrix (Figure 2.5C and D). The differences in MNP construction could explain some issues with how the conjugates interact with polymerase. The composition of the MNPs affects how they diffuse in

solution which is critical to enabled dNTPs to interact with polymerase. The stronger beam and detection of transmitted electrons gives TEM a better resolution. The stronger electron beam gives more capabilities, but in this case the electron beam degraded the polymer coatings on the MNPs making it challenging to get a representative image (Figure 2.5).

TEM-EDS was also attempted. Energy dispersive X-ray spectroscopy (EDS) enables analysis of elemental composition of a sample. It uses incident electrons to knock out an inner shell electron creating an electron hole with a positive charge. An electron from a higher energy shell relaxes to the positively charged hole releasing energy in the form of an X-ray. Elements have unique energies of their released electrons which can be detected to determine composition. Similar to other techniques, we were looking for phosphorus signal here to confirm conjugation. EDS did not give great signal for phosphorus. This is probably due to greatest signals coming from cobalt, iron and carbon such that the composition of the MNP was masking the phosphorus signal that was in much less quantity. It also did not help that polymer coatings were degraded by the beam.

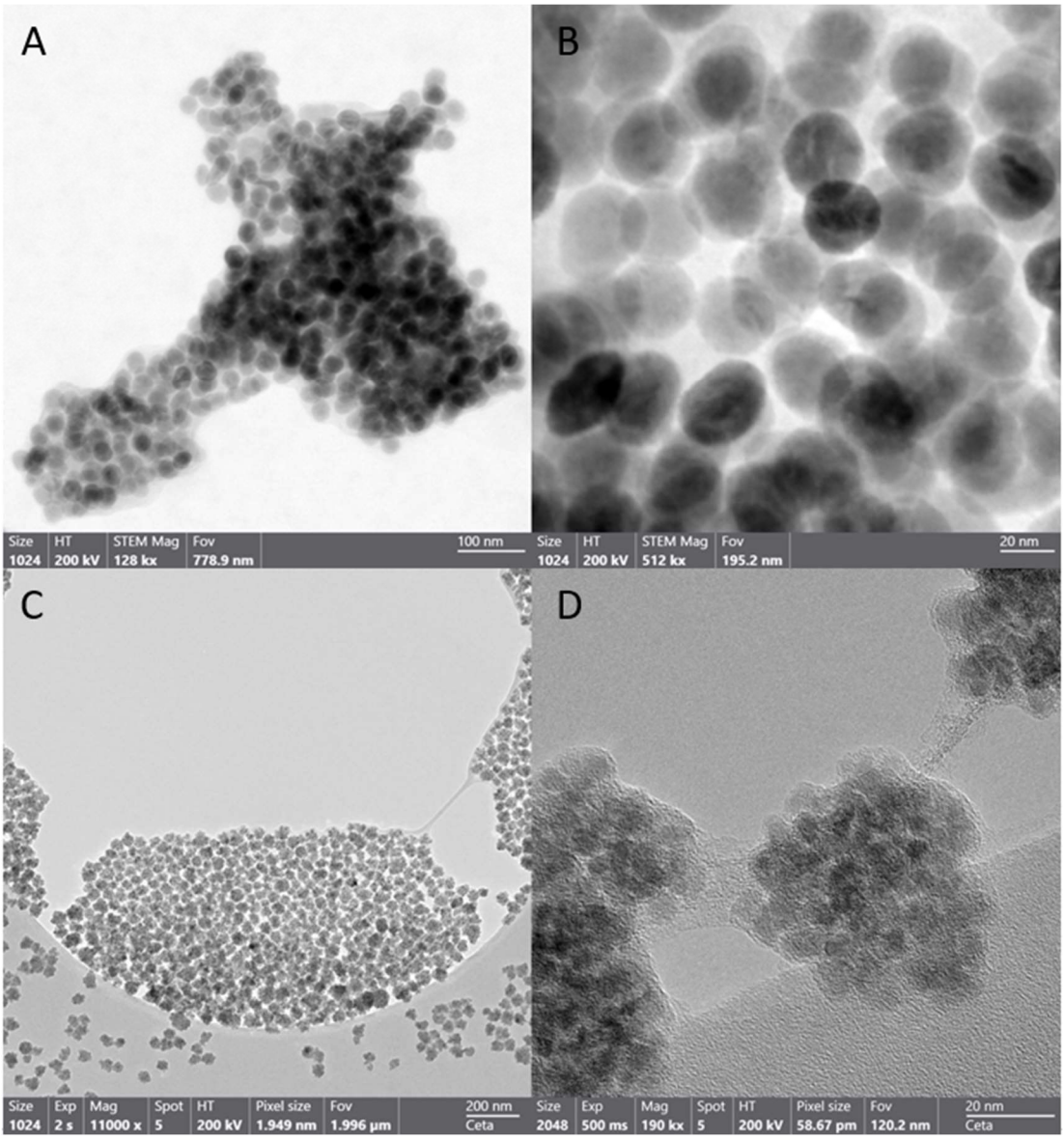

Figure 2.5: Transmission electron microscopy results: **(A)** Azide functionalized MNPs with 778.9 nm FOV. **(B)** Azide MNPs at 195.2 nm FOV. Images of azide MNPs show good size uniformity, and they look like they are made of solid chunks of metal with polymer coating. They were used in the PEG conjugation method. **(C)** Carboxyl terminated MNPs at FOV of 1.996 µm. **(D)** Carboxyl MNPs at 120.2 nm FOV. Images of carboxyl MNPs show smaller (<10 nm) particles held together with polymer matrix. These were used in EDC method.

2.4 Conclusions

The methods of attachment behaved similarly in terms of characterization. For the EDC method, we realized that many of the experiments were run with carboxyl MNPs rather than amine MNPs. After getting more information from the manufacturer of the MNPs, we learned that there is bovine serum albumin (BSA) in the MNP coating (OceanNanotech). BSA has free amines which more likely reacted with the dNTP phosphate to attach the dNTPs and MNPs (Figure 2.1). The EDC method seemed to work better with carboxyl beads rather than amine beads. For both techniques, nanoparticles from OceanNanotech worked best and had good size uniformity.

The various characterization techniques were sufficient to give confidence that the nucleotides were bonded to the nanoparticle. However, quantification of the concentration or percent yield remains unattainable. FTIR is often used for similar characterization but was inconclusive for these experiments. Still, many of the peaks were identifiable to give some confidence that the correct product was made (Figure 2.2). XPS gave greater affirmation that the reactions were successful. The unreacted MNPs show no phosphorus signal, however the reacted dNTP-MNP conjugates show phosphorus signaling the presence of nucleotides (Figure 2.3).

Quantifying the radius of the nanoparticle using EM was proposed to confirm conjugation, but this was not successful due to the large distribution of nanoparticle sizes. SEM was attempted first and showed that the nanoparticles being used were not homogenous in size. Both nanoparticle types imaged with TEM showed good size uniformity. The azide MNPs look like they are solid pieces of metal, whereas the carboxyl MNPs are smaller particles (<10 nm) held together in a polymer matrix

(Figure 2.5). In Chapter 3, we discuss experiments interacting the dNTP-MNP conjugates with polymerase. The composition of the MNPs could explain some of the interactions and issues that arose.

XPS gave confirmation of phosphorus in the dNTP-MNP conjugates confirming the presence of dNTP in the MNP samples. Although the reaction was not quantified, there was enough confirmation of dNTP-MNP conjugation to move forward with PCR and testing the conjugation products with a polymerase.

Chapter 3: Polymerase Chain Reaction

3.1 Introduction

Polymerase chain reaction (PCR) is a three-step reaction that creates millions of copies of a strand of DNA. The first step – Denature – heats the double stranded template DNA to separate it into two single strands. The second step – Anneal – is where the primers attach to the single stranded templates and DNA polymerase (Phusion) attaches to the template-primer complex. The third and final step – Extend – is the actual step where the DNA is copied. The polymerase attaches nucleotides from the solution to the template strand to complete a new double strand. This three-step cycle is repeated (usually for 40 cycles).

qPCR (quantitative PCR) differs from regular PCR in that the DNA amplification can be seen in real time. It uses a fluorophore (SYBR Green) to bind to the newly synthesized double-stranded DNA and fluoresces. The qPCR machine measures fluorescence at the end of each cycle and records it. At the end of the cyclic process, a melt curve can be run to determine the melt temperature of the DNA strands. If all curves denature at the same temperature, then it is reasonable to say that they are the same strand.

PCR and qPCR assays generally use dNTPs in solution to amplify sample DNA. Samples are often unknown and generating a greater sample size with PCR enables more complete characterization and understanding of the sample. In this case qPCR is used to analyze known DNA samples using the dNTP-MNP conjugates in place of

unconjugated dNTPs. This enables assessment of how MNPs affect nucleotide-polymerase interaction, and it can also show that nucleotide-MNPs are attached.

3.2 Methods & Materials

Commercial PCR master mixes generally include all four dNTPs. Thus, multiple master mixes had to be made to account for the varying dNTP combinations. Appendix B shows master mix set up values. The components of the PCR mix include Phusion buffer (SigmaAldrich), forward and reverse primers (Integrated DNA Technologies (IDT)), with matching template (IDT). For these reactions, Phusion high fidelity polymerase (ThermoFisher) was used as the enzyme. Since qPCR was being run, a fluorophore was needed, and SYBR Green (MilliporeSigma) was the fluorophore added. Nuclease free water or glycerol was used to dilute the samples and bring them to the desired volume.

For the PCR, BioRad CFX Connect Real-Time PCR Detection System was used both as thermocycler and to review qPCR data. The experimental setup included a denature an initial denature at 98 °C, cyclical denature also at 98 °C, then anneal and extension at 56 °C. The cyclical denature and anneal and extension steps continued for 40 cycles. After the amplification, the samples were gradually heated to develop a melt curve. The temperatures and times for the final reaction is shown in Table 3.1. From that table, all the temperatures remained the same throughout all experiments, but the annealing/extension time changed.

Table 3.1 | Experimental Parameters for Thermocycler

Step	Temp °C	Time (s)	# Cycles
Enzyme Activation	98	30	1
Denaturation	98	5	40
Annealing/Extension	56	60	40
Melt 1	98	15	1
Melt 2	60	60	1
Melt 3	98	15	1

Table 3.2 shows how some of the parameters developed as the project proceeded. The dNTPs in the samples were some combination of the MNP-dNTP conjugates and commercially purchased dNTPs. For the initial trials, experiments were run with three of the four nucleotides in solution being commercially purchased from ThermoFisher (experiment types 1-3). The fourth nucleotide was one of the MNP-dNTP conjugates from Chapter 2. This initial approach was selected to as to have only one independent variable. After successes with these experiments only varying one dNTP, we moved forward with testing all four dNTP-MNPs together with no commercially purchased dNTPs (experiment types 4,5). The solvent for the reaction also evolved as experimental results were acquired. The first trials were done in water, and subsequent trials experimented with different concentrations of glycerol in water (v/v) (experiment types 2-5). The anneal/extension times were increased to account for increase in viscosity from the glycerol. The template concentration was increased for experiment type 4 for trying all four dNTP-MNPs together. Experiment type 5 was a standard curve, so it has varying template concentration.

Table 3.2 | qPCR Experimental Progression

Experiment Type	1	2	3	4	5
dNTP-MNPs	1	1	1	4	4
Purchased dNTPs	3	3	3	0	0
Anneal/Extension (s)	30	30	60	60	60
Glycerol/Water% (v/v)	0	33	33	25	25
Template Conc. (pM)	0.1	0.1	0.1	10	vary

To ensure the validity of the experiments, there were a number of experimental controls. The positive controls had all four dNTPs purchased commercially. This was to show how the PCR would perform with unmodified dNTPs. There were also three types of negative controls. First, there were no-template controls that did not have template DNA, so there was nothing to replicate. Second, supernatant controls used the supernatant, but no MNPs, from the dNTP being tested. These samples were prepared by centrifuging the aqueous dNTP-MNP sample at 10000 rpm for 12 minutes to concentrate the MNPs at the bottom of the tube. 100 µl of the supernatant was removed by pipette and used as that dNTP for the supernatant control in the qPCR mix. This was to further confirm that the dNTPs were chemically bonded to the MNPs, not just in solution. If signal arose from these supernatant control samples, that would signify issues with purification of the dNTP-MNP conjugates and could imply that the dNTPs were just in solution but not chemically bonded to the MNP. Having no signal from these controls, combined with positive signal from the experimental samples, would show that the dNTPs are chemically bonded to the MNP and are not just mixed in solution. Finally, the third negative control were samples completely lacking one dNTP.

To confirm the amplification product, the samples were run on a gel. The gel, a 4% agarose in TBE buffer, was constructed using the Sub-Cell GT Agarose Gel Electrophoresis Systems DNA Gel Preparation protocol from BioRad. The samples included DNA ladder (ThermoFisher), three replicates of the qPCR product, and a positive control which was the diluted template DNA. For the three replicates of the qPCR product, one was just the product from the qPCR well. The second took all the contents of the qPCR well and purified them using PureLink PCR Purification Kit from ThermoFisher. The third magnetically separated the beads from the supernatant of the product, and then used the PCR Purification Kit.

3.3 Results and Discussion

3.3.1 qPCR For Experiment Types 1-3

The initial qPCR experiments were run varying just one dNTP. Three of the dNTPs in each experiment were purchased commercially, while the fourth was a dNTP-MNP conjugate. After tuning the experimental conditions, the first experiment type 1 qPCR trial with success showed signal from the positive control and from 3 of the EDC samples (Figure 3.1). The melt curve (Figure 3.1B) shows that all the amplified products melted at the same temperature. This signifies that they are the same product.

In this experiment, there were 12 experimental samples, and only 3 of them showed amplification. All three of the successful samples were dNTPs attached to MNPs using the EDC conjugation method. None of the PEG samples worked. We noticed that the MNPs were sinking to the bottom of the qPCR wells. Theoretically, the polymerase and other dNTPs are well suspended in solution, so having the MNPs all concentrated at the bottom minimizes the possibility of that dNTP interacting with polymerase.

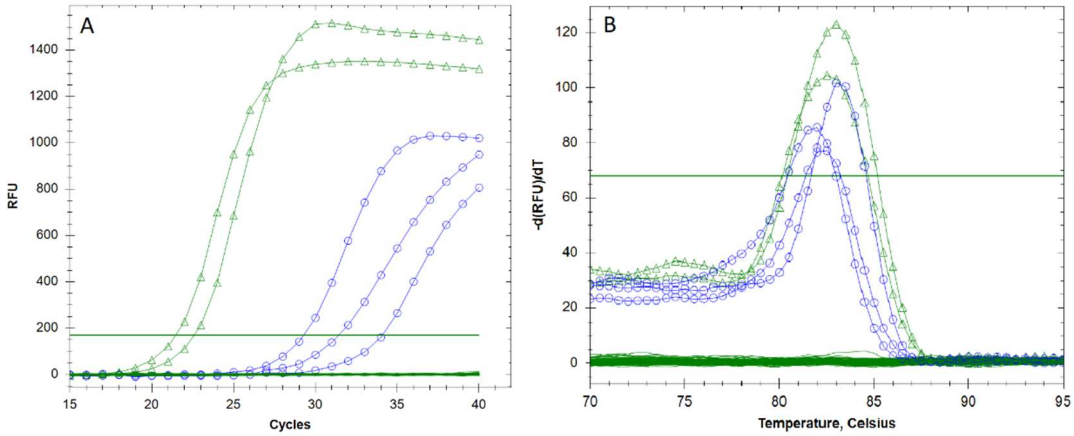

Figure 3.1: Initial qPCR results: **(A)** shows amplification signal from both positive controls (Δ, green) and 3 experimental controls (○, blue). **(B)** is the melt curve showing all amplified products melting at same temperature.

To counteract this sedimentation of the MNPs, experiments were run with various concentrations of glycerol in water as the solvent for the reaction. It was not possible to develop a qPCR mixture with 100% glycerol because some of the reagents in the mixture were purchased in aqueous solutions. Still, some of the higher concentrations of glycerol did not show the best amplification. This is probably due to increased viscosity hindering diffusion and therefore limiting the interaction between reactants. The best performing solvent ratio was 33% glycerol in water by volume.

These experiments with glycerol (experiment type 2) still did not achieve amplification signal from all experimental samples. As stated above, increasing the viscosity of the solution reduces diffusion. To account for this, the anneal/extension time was increased from 30 s to 45 s. This increase showed better results, so the process time was increased again to 60 s. With the extended time for diffusion, all of the EDC variants showed amplification from at least one replicate. The PEG samples however,

still had limited success. Only 2 of 8 samples showed any signal. For this reason, it was decided to only continue with the EDC samples.

The lack of success for the PEG dNTP-MNPs could be due to the functionalization. Perhaps there were not as many dNTPs attached to the MNP. It also could be due to the composition of the MNP. The MNPs used for the PEG method were solid chunks of metal compared to the much smaller particles for the EDC method resulting in a higher amount of bead aggregation. Also, the greater density for the PEG MNPs may also cause greater sedimentation and contribute to the lack of success. Finally, the PEG samples have a PEG linker between the dNTP and MNP. This was initially proposed to give the dNTP some flexibility and separation from the MNP so that the polymerase could cleave the dNTP from the MNP. Maybe this addition had adverse effects making it difficult for the polymerase to cleave the nucleotide.

For experimenting with just the EDC samples, Figure 3.2 shows the qPCR results for the updated experimental parameters of 33% glycerol/water solvent and 60 s anneal/extension time. These results show all 4 EDC samples with amplification. The Cq values indicate the cycle when the amplification quantity crossed the threshold. This is done by the fluorescence measurement at the end of each cycle measuring the fluorophores attached to DNA and providing relative fluorescence units (RFU) as a function of the cycles (Figure 3.2). The log plot gives a better visualization of the Cq value where the amplification curve crosses the threshold.

The greater viscosity with the glycerol minimizes sedimentation of the reactants and allows more interaction between polymerase and dNTP-MNPs. However, the glycerol solution also changes the melt curve. The peaks shift and do not match up.

This could indicate that they are not all the same DNA sequence, but it has been shown that polyols such as glycerol can shift melt curves [28]. After adding glycerol to the solvent, the melt curves were unreliable to confirm qPCR product identity.

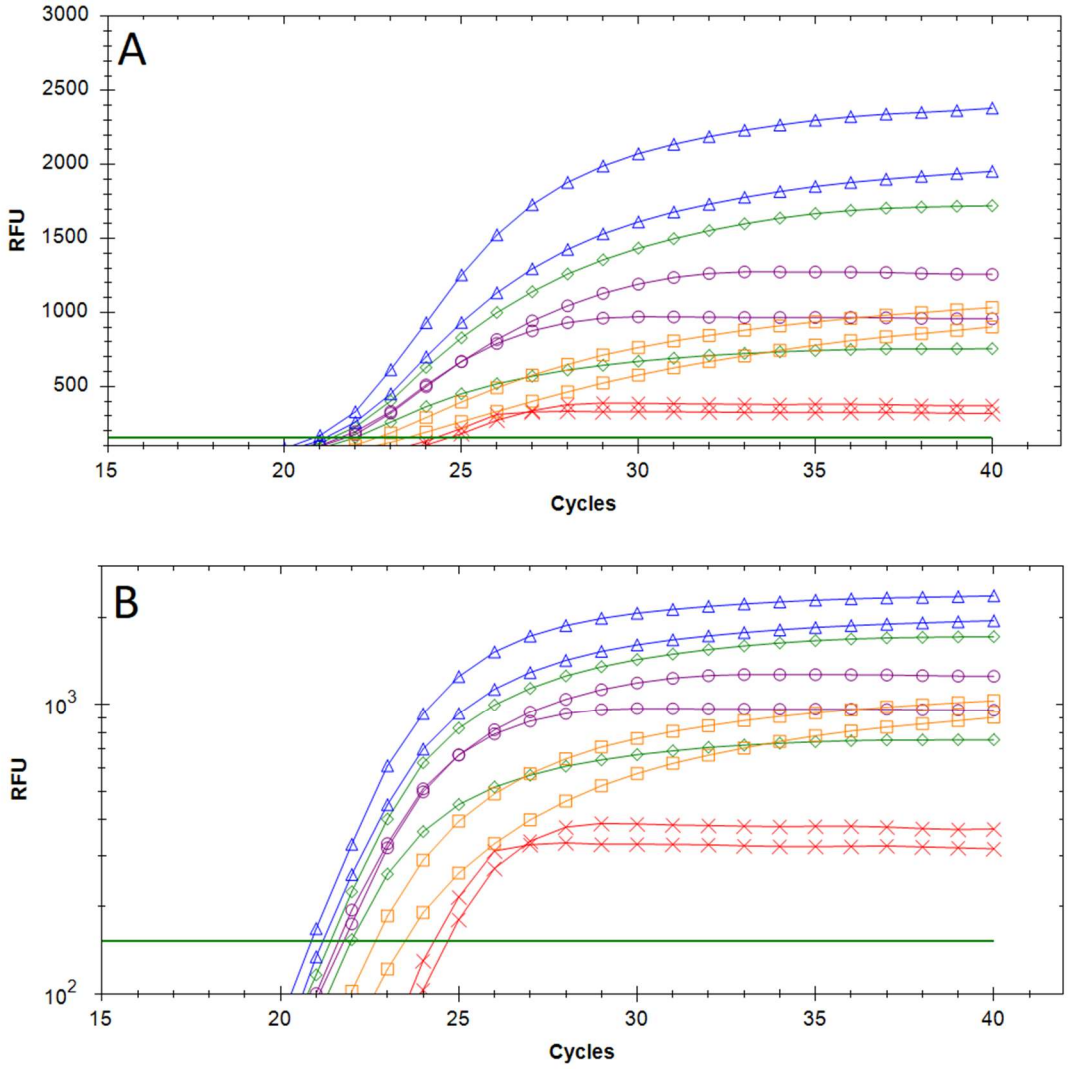

Figure 3.2: qPCR results for 33% Glycerol/Water solution. Each sample has one dNTP-MNP conjugate. Both the raw **(A)** and log **(B)** plots show all samples amplified with Cq between 20 and 25 cycles. Positive Control (Δ, blue), dGTP-MNP (◇, green), dCTP-MNP (○, purple), dATP-MNP (□, orange), dTTP-MNP (×, red).

3.3.2 qPCR For Experiment Types 4-5

After having success with varying one dNTP in the qPCR experiments, we moved on to experiment type 5 testing all 4 dNTPs in a single experimental solution so that the only dNTPs in each sample were dNTP-MNP conjugates. Because all the dNTP-MNPs were in aqueous solutions, and other reactants were also aqueous, it was difficult to get a 33% glycerol/water solution, so this trial was run in 25% glycerol/water. Anticipating some issues, the template concentration for this experiment was increased from 100 fm (0.1 pm) to 10 pm (Table 3.2). All six samples in the experiment were identical, and all showed similar amplification (Figure 3.3).

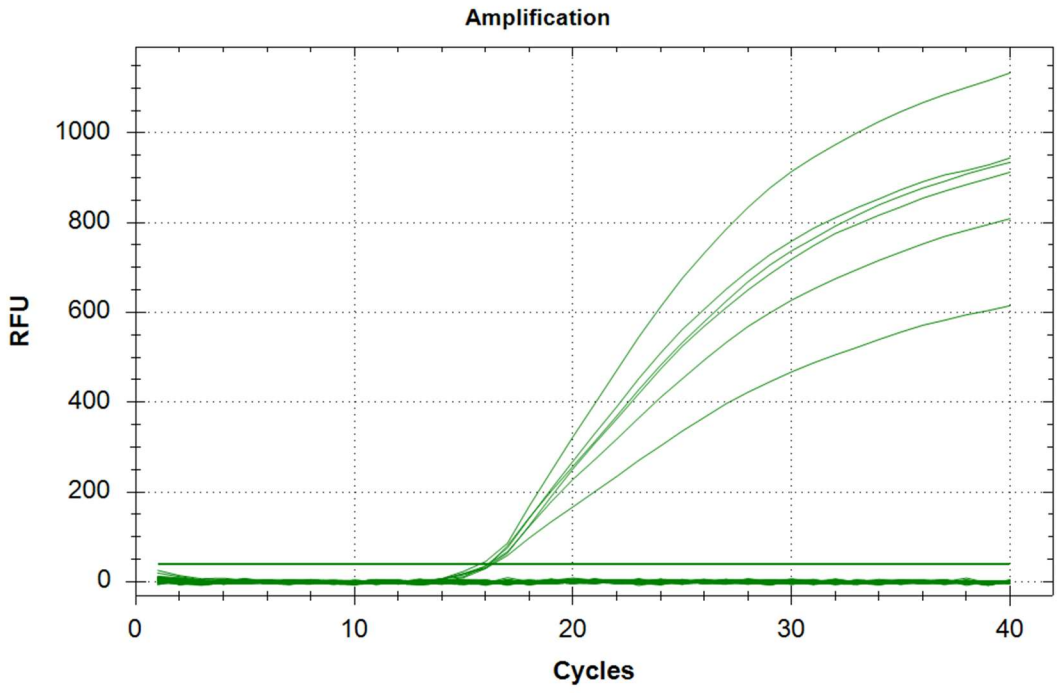

Figure 3.3: qPCR results for all dNTPs in sample being dNTP-MNP conjugates (experiment type 4). All samples are identical.

All four dNTP-MNPs in the same sample worked significantly better than expected. This could be attributed to the increased template concentration. Theoretically, the DNA concentration will double after each cycle, so starting with 100x more DNA would help reach the threshold much earlier. This is evident by the Cq values close to 16 cycles for the four dNTP-MNPS compared to the Cq values close to 22 cycles when testing only one dNTP-MNP.

To calculate the efficiency of this reaction, a standard curve was conducted on these samples (Figure 3.4). This confirmed the previous results that the four dNTP-MNP conjugates can function in the same sample as each other, but they also showed good amplification for the lower concentrations. It is not understood why this works much better than the experiments with only one dNTP-MNP. It is possible that with all dNTPs in solution attached to MNPs, they all have the same rate of diffusion and have the same probability of interacting with the polymerase. With only one dNTP attached to an MNP, the dNTP-MNP system is significantly heavier and larger than the dNTPs in solution. Therefore, the dNTP attached to the MNP will have less interaction with polymerase compared to the other dNTPs.

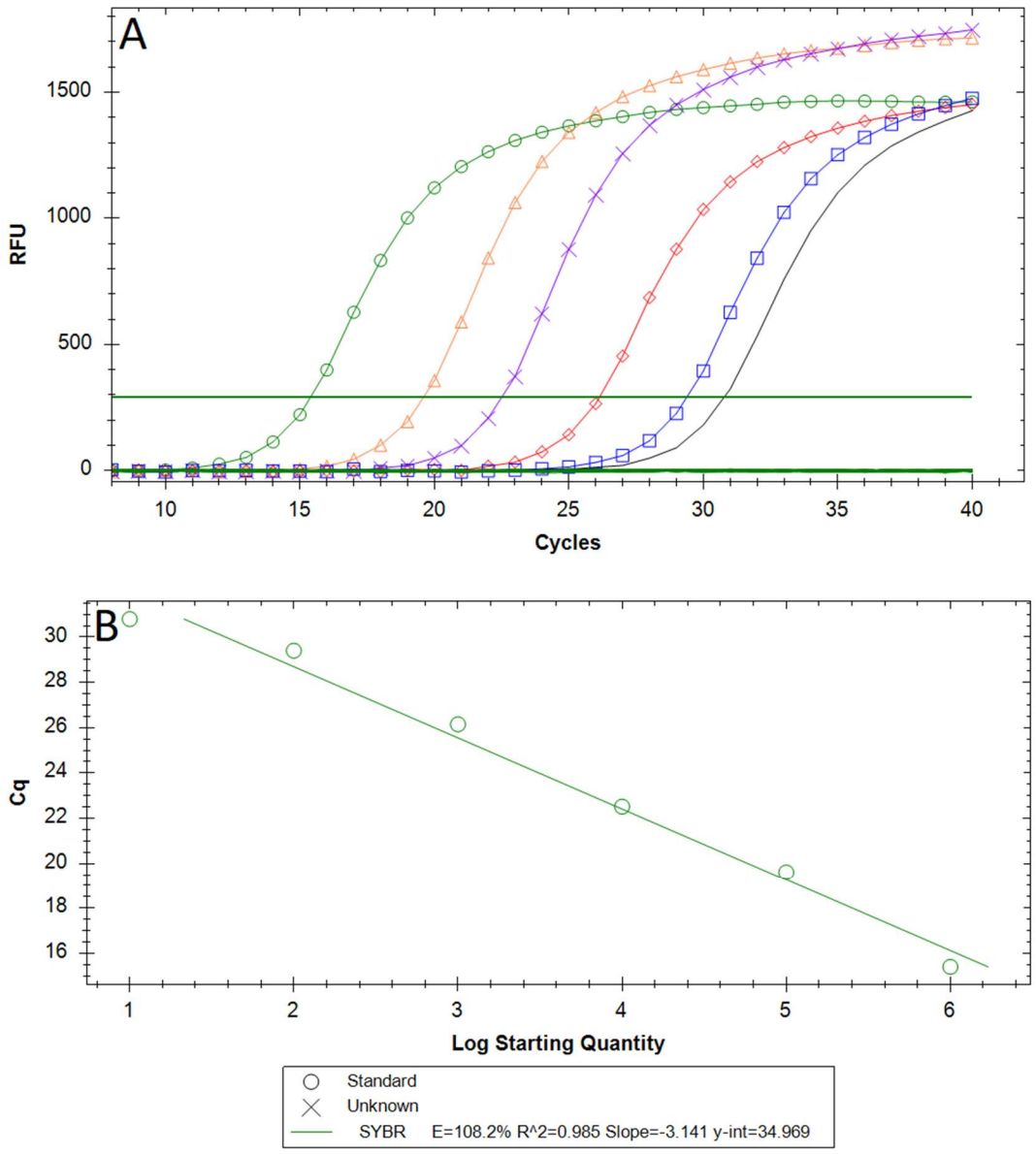

Figure 3.4: qPCR standard curve results for experiment type 5. **(A)** Amplification curve. Each sample is identical except for the varying template concentration. 10 pm (○, green), 1 pm (Δ , orange), 100 fm (×, purple), 10 fm (◇, red), 1 fm (□, blue), 0.1 fm (-, black). **(B)** Standard curve showing efficiency and R^2 values for this reaction.

The standard curve was the result of plotting the log of the starting template concentration vs. the Cq values. Desirable qPCR experiments produce linear standard curves with reaction efficiency between 90-110% and R^2 values >0.980 [29]. The efficiency of the reaction was calculated using the BioRad analysis software, and follows

$$\%\, Efficiency = E = 100 \times (10^{-\frac{1}{slope}} - 1) \tag{3.1}$$

The experimental standard curve data demonstrated an efficiency of 108.2% and an R^2 value of 0.985 (Figure 3.4). Both of these values are comparable to other PCR values and are within acceptable ranges for successful qPCR [29]. This shows that attaching dNTP to an MNP does not inhibit polymerase interaction with the dNTP.

Producing an E value > 100% is not uncommon. Key contributors to unreasonably high efficiency are inhibitors and pipetting mistakes [30]. Polymerase inhibition generally results from some contamination in the sample inhibiting amplification. This creates a lower slope which artificially increases the efficiency. Similarly, pipetting errors can either decrease reagents for the higher template concentrations or decrease reagent concentrations for the more diluted samples. Both effectively decrease the slope increasing the calculated efficiency. Still, E values between 90 and 110% are generally accepted as withing 10% deviation from ideal.

3.3.3 Gel Electrophoresis

Although there was amplification, as shown by the qPCR data, gel electrophoresis was run to confirm the identity of the amplified qPCR product. It was desired to check the length of the PCR products because the melt curves did not match up as stated previously. Gel electrophoresis (GE) is a standard method for confirming qPCR products or determining size of DNA strands. It uses an ionic current to propel DNA strands through an agarose gel based on the negative charge of the DNA. The DNA strands move from the negative electrode where they are injected into wells to the positive electrode. This method separates DNA strands based on their sizes. The smaller DNA strands will move further along the gel since they are smaller.

In this case, gel electrophoresis was used to show that the product from the qPCR reactions is the same length as the template DNA – that the qPCR with the dNTP-MNPs successfully amplified the complete template strand. The positive control for this experiment was just the template strand from the qPCR reaction. The results show that the qPCR samples are the correct DNA strand. All three samples showed up at the same length (~100bp) as the template (Figure 3.5). However, the signal from the purified samples was significantly less than that of the unpurified sample; there is thus a lot of sample loss from the purification process.

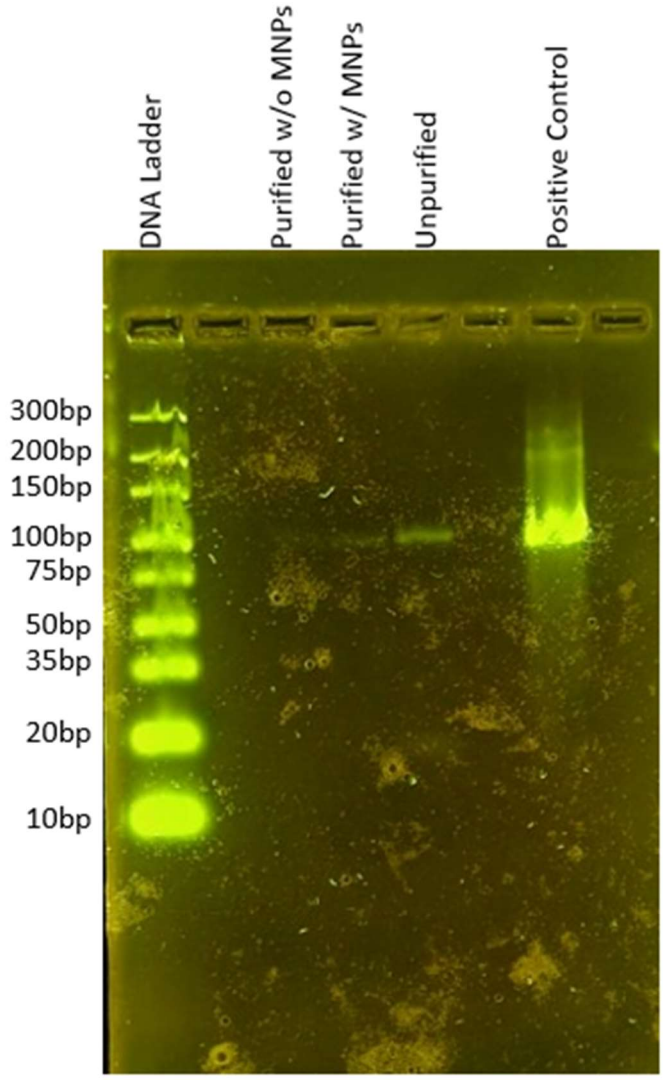

Figure 3.5: Gel Electrophoresis of qPCR products. Lanes are labeled with samples: DNA Ladder, Purified w/o MNPs, Purified w/ MNPs, Unpurified, Positive Control. Results show the amplification products match the positive control at ~100bp.

3.4 Conclusions

The initial reactions ran in an aqueous solution with a 30 s anneal and extension time. They showed amplification of the EDC samples, but not of the PEG samples. The melt curve showed all samples that amplified melted at the same temperature which confirmed the correct product was created. It was noted that the MNPs were sedimenting to the bottom of the PCR wells. This could account for the minimal interaction between the dNTPs and polymerase. To overcome this limitation, solutions of different concentrations of glycerol in water were studied.

The first tests with glycerol had improvements, but the viscous fluid limits diffusion. So the anneal/extension time was increased from 30 s first to 45 s and then to 60 s. Both increases in time improved amplification. The EDC samples showed significant improvement with a 33% glycerol in water solution and 60 s anneal/extension time (Figure 3.2). However, the PEG samples also showed improvement, but not significant or as good as the EDC samples, so the EDC samples were chosen to continue the experiment.

For the experiments testing all four dNTP-MNPS in each sample, the template concentration was increased to 10 pM to give the experiment more chance of working. This seemed to work better than one dNTP-MNP conjugate experiments. This could be due to all four dNTPs diffusing at similar rates rather than the one experimental dNTP being significantly slower than the other three. A standard curve was generated to characterize the polymerase-dNTP interaction (Figure 3.4). The R^2 value (0.985) and efficiency (E=108.2%) show that this interaction performs similarly to accepted PCR

reactions. This signifies that the dNTP attachment to MNP does not hinder the activity of the polymerase.

Due to the melt curve shift with the glycerol solution, gel electrophoresis was conducted to confirm the PCR product (Figure 3.5). The purification methods attempted seemed to lose a lot of product. However, all experimental samples matched the positive control showing that the PCR worked, and the correct product was created.

Chapter 4: Final Summary

Two methods were attempted to attach dNTPs to MNPs. The EDC method involved attaching dNTP directly to the MNP surface, and the PEG method used a PEG linker to create some separation between the dNTP and MNP. Both the PEG method and EDC method showed success in conjugation. With various characterization and imaging methods, the samples showed conjugation of dNTP to MNP although quantification of conjugation was thus far unattainable.

Both samples were then tested with polymerase to determine how the MNP affects the polymerase-dNTP interaction. Here the dNTP-MNPs that were formed using the EDC method performed significantly better. Using a more viscous solvent such as glycerol minimized the sedimentation of the MNPs and allowed for greater interaction between the polymerase and dNTPs. MNP functionalization does not inhibit dNTP-polymerase interaction. The next steps for this project are developing unique MNP types so that each of the four bases has a unique label. This will then be incorporated with our graphene sensor to be tested as a DNA sequencing system.

Bibliography

1. WATSON, J. D., and F. H. CRICK. “Molecular Structure of Nucleic Acids: A Structure for Deoxyribose Nucleic Acid.” *Nature*, vol. 171, no. 4356, 1953, pp. 737–738., https://doi.org/10.1038/171737a0.
2. Brody, Lawrence. “Nucleotide.” *Genome.gov*, 10 May 2022, https://www.genome.gov/genetics-glossary/Nucleotide.
3. Bee, Callista, et al. “Molecular-Level Similarity Search Brings Computing to DNA Data Storage.” *Nature Communications*, vol. 12, no. 1, 2021, https://doi.org/10.1038/s41467-021-24991-z.
4. Moore, G.E. “Cramming More Components onto Integrated Circuits.” *Proceedings of the IEEE*, vol. 86, no. 1, 1 Jan. 1998, pp. 82–85., https://doi.org/10.1109/jproc.1998.658762.
5. Schaller, R.R. “Moore's Law: Past, Present and Future.” *IEEE Spectrum*, vol. 34, no. 6, June 1997, pp. 52–59., https://doi.org/10.1109/6.591665.
6. Gymrek, Melissa, et al. “Identifying Personal Genomes by Surname Inference.” *Science*, vol. 339, no. 6117, 2013, pp. 321–324., https://doi.org/10.1126/science.1229566.
7. Peikon, Ian D., et al. “Using High-Throughput Barcode Sequencing to Efficiently Map Connectomes.” *Nucleic Acids Research*, vol. 45, no. 12, 2017, https://doi.org/10.1093/nar/gkx292.
8. Shendure, Jay, et al. “DNA Sequencing at 40: Past, Present and Future.” *Nature*, vol. 550, no. 7676, 2017, pp. 345–353., https://doi.org/10.1038/nature24286.
9. Holley, Robert W., et al. “Structure of a Ribonucleic Acid.” *Science*, vol. 147, no. 3664, 1965, pp. 1462–1465., https://doi.org/10.1126/science.147.3664.1462.
10. Wu, Ray, and Ellen Taylor. “Nucleotide Sequence Analysis of DNA.” *Journal of Molecular Biology*, vol. 57, no. 3, 1971, pp. 491–511., https://doi.org/10.1016/0022-2836(71)90105-7.
11. Gilbert, Walter, and Allan Maxam. “The Nucleotide Sequence of the *Lac* Operator.” *Proceedings of the National Academy of Sciences*, vol. 70, no. 12, 1 Dec. 1973, pp. 3581–3584., https://doi.org/10.1073/pnas.70.12.3581.
12. Sanger, F., et al. “DNA Sequencing with Chain-Terminating Inhibitors.” *Proceedings of the National Academy of Sciences*, vol. 74, no. 12, 1977, pp. 5463–5467., https://doi.org/10.1073/pnas.74.12.5463.
13. Maniatis, Tom, et al. “Chain Length Determination of Small Double- and Single-Stranded DNA Molecules by Polyacrylamide Gel Electrophoresis.” *Biochemistry*, vol. 14, no. 17, 1 Aug. 1975, pp. 3787–3794., https://doi.org/10.1021/bi00688a010.
14. Smith, Lloyd M., et al. “Fluorescence Detection in Automated DNA Sequence Analysis.” *Nature*, vol. 321, no. 6071, 1986, pp. 674–679., https://doi.org/10.1038/321674a0.
15. Connell, Charles, et al. "Automated DNA-sequence analysis." *BioTechniques* 5.4 (1987): 342

16. Morozova, Olena, and Marco A. Marra. “Applications of next-Generation Sequencing Technologies in Functional Genomics.” *Genomics*, vol. 92, no. 5, 2008, pp. 255–264., https://doi.org/10.1016/j.ygeno.2008.07.001.
17. Voelkerding, Karl V, et al. “Next-Generation Sequencing: From Basic Research to Diagnostics.” *Clinical Chemistry*, vol. 55, no. 4, 2009, pp. 641–658., https://doi.org/10.1373/clinchem.2008.112789.
18. Levene, M. J., et al. “Zero-Mode Waveguides for Single-Molecule Analysis at High Concentrations.” *Science*, vol. 299, no. 5607, 2003, pp. 682–686., https://doi.org/10.1126/science.1079700.
19. Eid, John, et al. “Real-Time DNA Sequencing from Single Polymerase Molecules.” *Science*, vol. 323, no. 5910, 2009, pp. 133–138., https://doi.org/10.1126/science.1162986.
20. “Illumina NovaSeq X Series.” *Production Scale, Ultra-High-Throughput Sequencers*, https://www.illumina.com/systems/sequencing-platforms/novaseq-x-plus.html.
21. “PacBio Revio: Long-Read Sequencing at Scale.” *PacBio*, 27 Oct. 2022, https://www.pacb.com/revio/.
22. Christiaens, P., et al. “EDC-Mediated DNA Attachment to Nanocrystalline CVD Diamond Films.” *Biosensors and Bioelectronics*, vol. 22, no. 2, 2006, pp. 170–177., https://doi.org/10.1016/j.bios.2005.12.013.
23. Serdjukow, S., et al. “Synthesis of γ-Labeled Nucleoside 5′-Triphosphates Using Click Chemistry.” *Chem. Commun.*, vol. 50, no. 15, 2014, pp. 1861–1863., https://doi.org/10.1039/c3cc48937j.
24. León, Andrea, et al. “FTIR and Raman Characterization of tio2 Nanoparticles Coated with Polyethylene Glycol as Carrier for 2-Methoxyestradiol.” *Applied Sciences*, vol. 7, no. 1, 2017, p. 49., https://doi.org/10.3390/app7010049.
25. Shukla, Nisha, et al. “FTIR Study of Surfactant Bonding to FePt Nanoparticles.” *Journal of Magnetism and Magnetic Materials*, vol. 266, no. 1-2, 2003, pp. 178–184., https://doi.org/10.1016/s0304-8853(03)00469-4.
26. Socrates, George. *Infrared and Raman Characteristic Group Frequencies: Tables and Charts*. John Wiley & Sons LTD, 2015.
27. K, Sunitha, et al. “Azide Telechelics Chain Extended by Click Reaction: Synthesis, Characterization, and Cross-Linking.” *Polymers for Advanced Technologies*, vol. 30, no. 2, 2018, pp. 435–446., https://doi.org/10.1002/pat.4483.
28. Henry, R. J., and K. Oono. “Amplification of a GC-Rich Sequence from Barley by a Two-Step Polymerase Chain Reaction in Glycerol.” *Plant Molecular Biology Reporter*, vol. 9, no. 2, 1991, pp. 139–144., https://doi.org/10.1007/bf02669207.
29. Taylor, Sean, et al. “A Practical Approach to RT-QPCR—Publishing Data That Conform to the MIQE Guidelines.” *Methods*, vol. 50, no. 4, 2010, https://doi.org/10.1016/j.ymeth.2010.01.005.
30. Svec, David, et al. “How Good Is a PCR Efficiency Estimate: Recommendations for Precise and Robust QPCR Efficiency Assessments.” *Biomolecular Detection and Quantification*, vol. 3, 2015, pp. 9–16., https://doi.org/10.1016/j.bdq.2015.01.005.

Appendix A: Supporting Information for Chapter 2

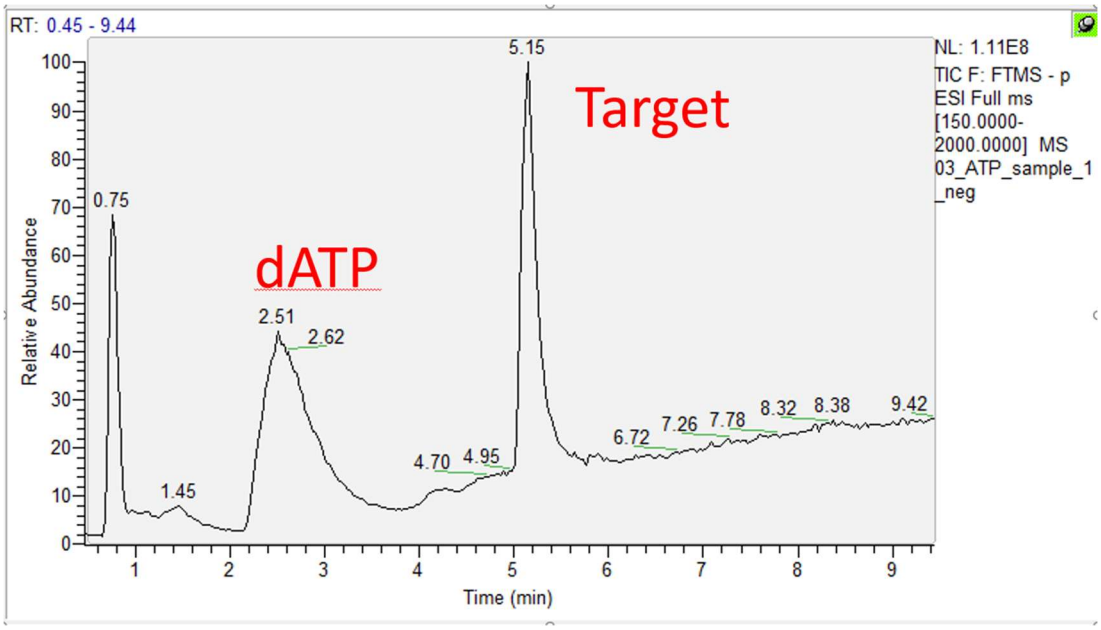

Figure A.1: HPLC data for dATP+PEG. Trace shows two large peaks that were labeled as unreacted dATP and dATP+PEG (Target) after MS of the samples (A.2).

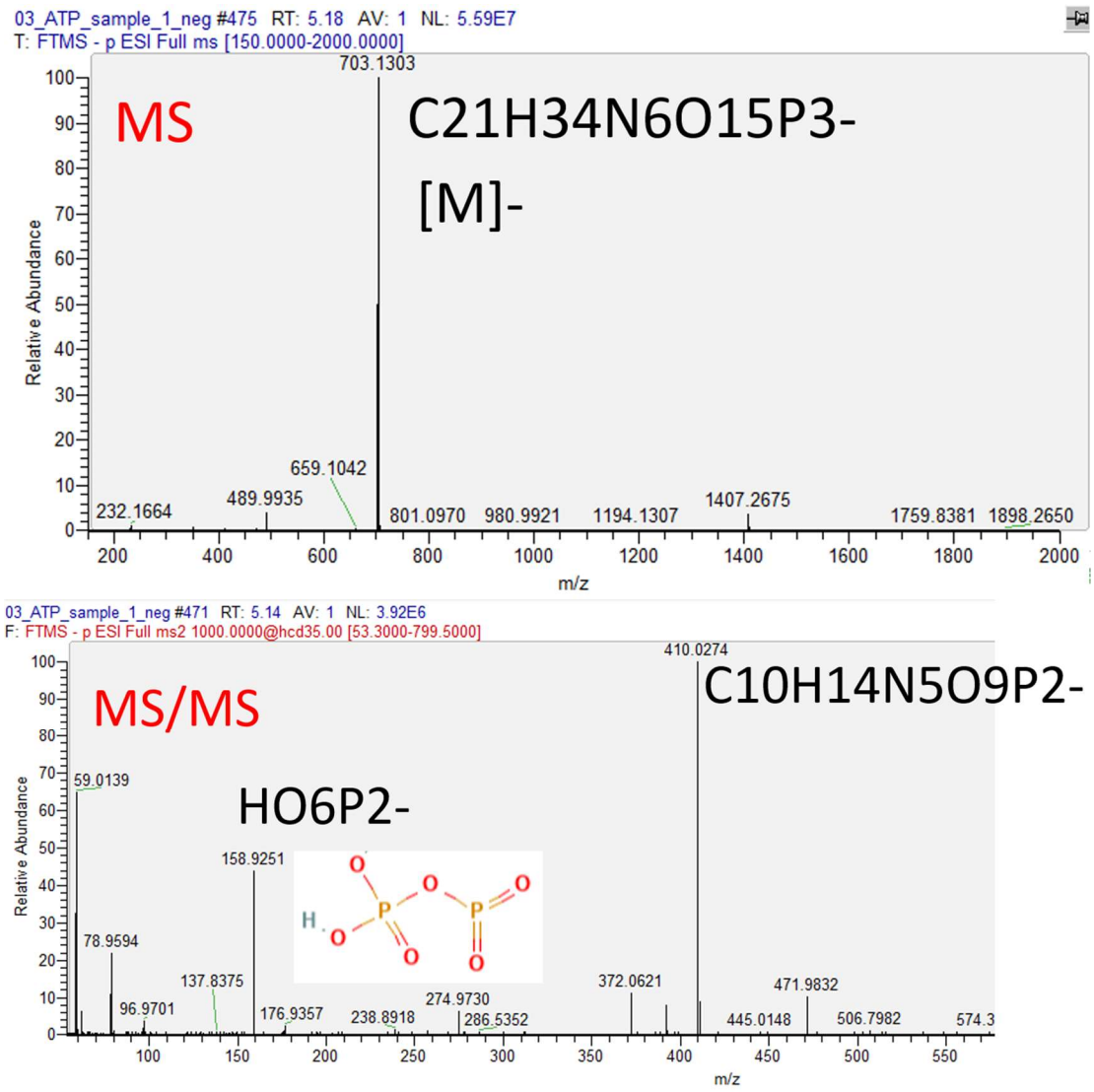

Figure A.2: MS (top) and MS/MS (bottom) showing desired product mass in MS and fragment data in MS/MS.

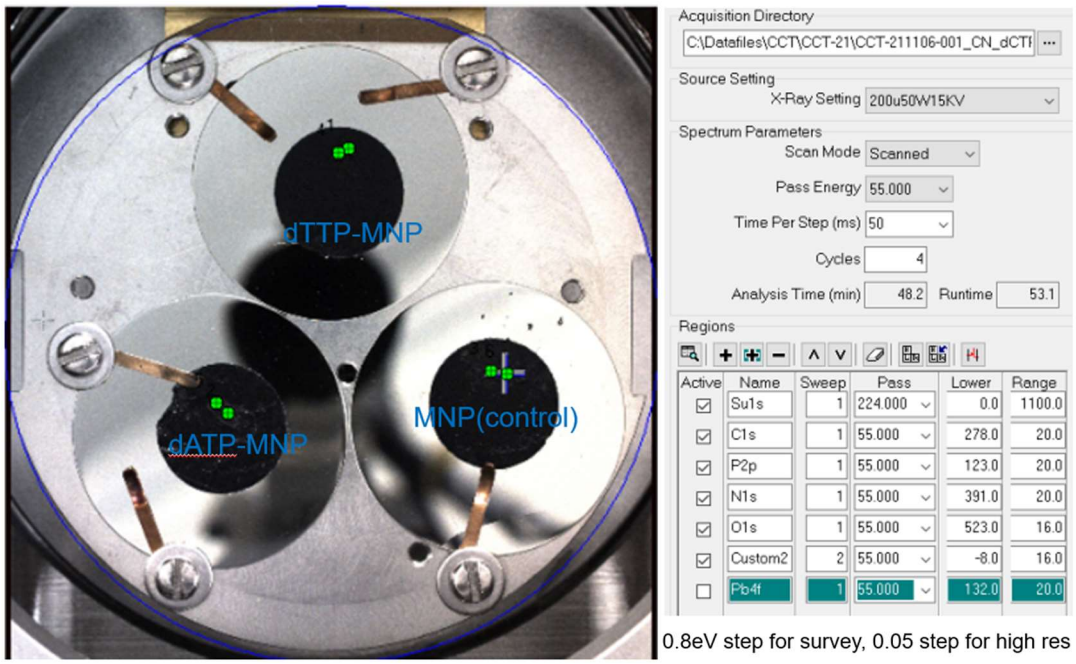

Figure A.3: XPS platen set up and experimental conditions.

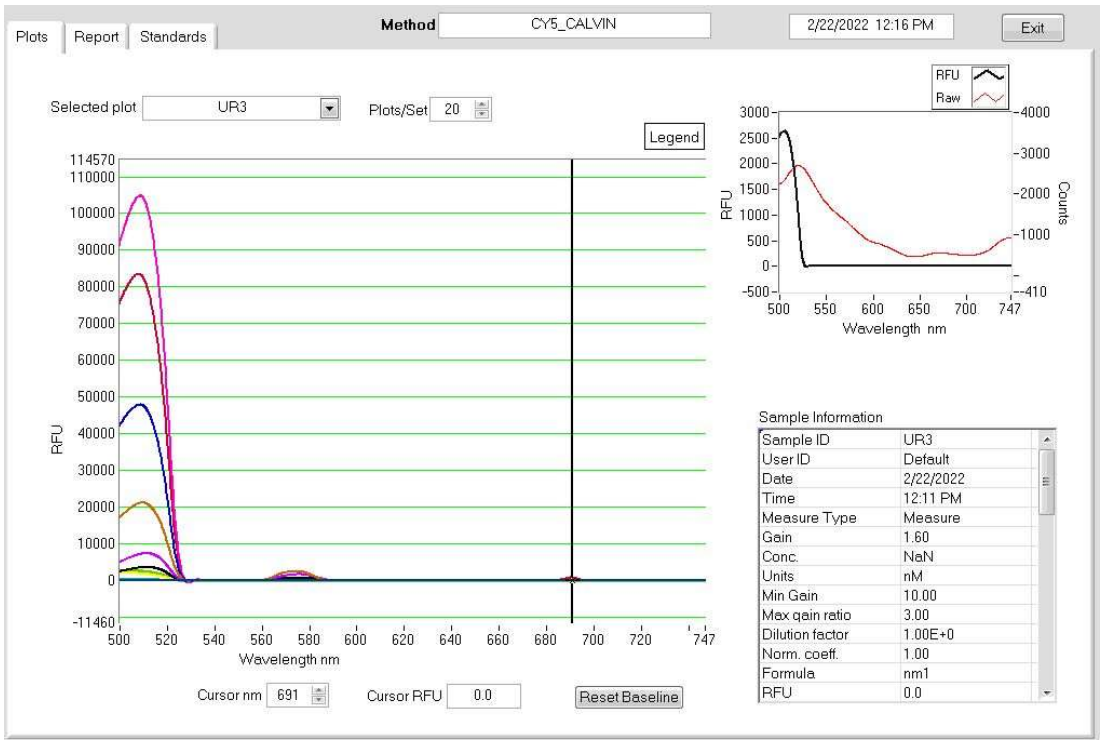

Figure A.4: Fluorescence data for Cy5. This was a control to show fluorescence of the unreacted Cy5. It should have excitation at 651 nm and emission at 670 nm, but was shifted left.

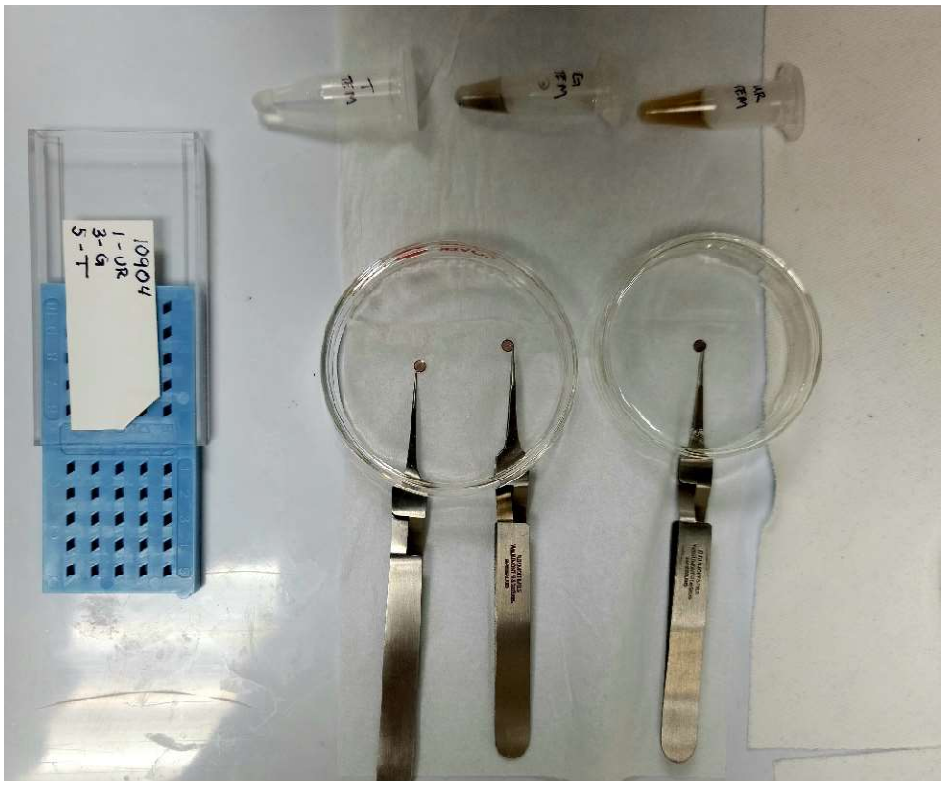

Figure A.5: TEM sample preparation drop casting samples onto grids and drying.

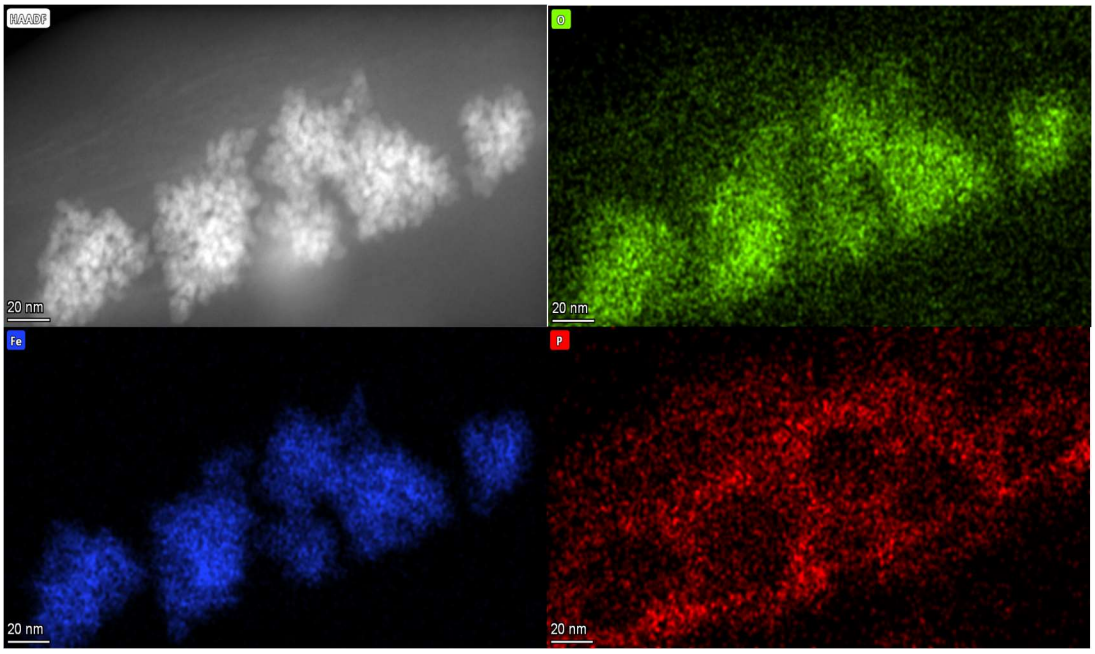

Figure A.6: TEM/EDS showing detection of high-angle dark field, oxygen (O), iron (Fe), Phosphorus (P) (Left to Right, Top to Bottom). Phosphorus images show rings of P signal coating MNPs.

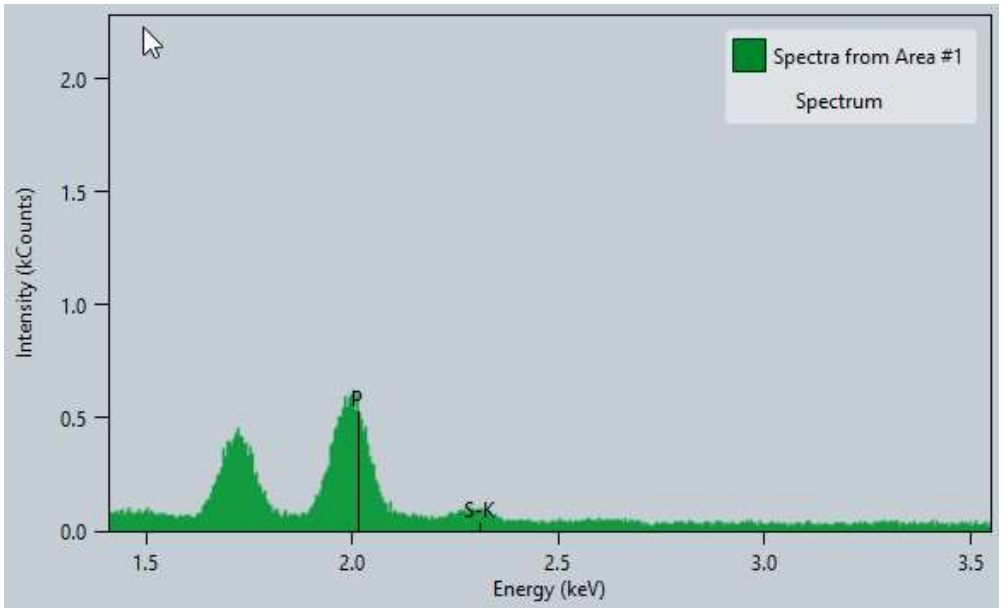

Figure A.7: TEM/EDS quantitative spectra data displaying P signal.

Appendix B: Supporting information for Chapter 3

B.1 – qPCR General Master Mix Setup (from Gemma Mendonsa)

Table B.1A: qPCR Master Mix with template (96 samples, 6 master mixes):

Component	Volume	Final concentration	Master Mix volume
5X Phusion HF Buffer (5x)	4 µL	1x	72 µL
10mM dNTPs (from separate components)	0.4 µL	200 µM each	7.2 µL
Forward primer (10uM) RandPosA Pforward	1 µL	0.5 µM	18 µL
Reverse primer (10uM) RandPosA PReverse	1 µL	0.5 µM	18 µL
Template DNA (RandPosA top+bottom)	1 µL	0.1-10 ng	18 µL
Phusion™ High–Fidelity DNA Polymerase	0.2 µL	0.02 U/µL	3.6 µL
10X SYBR Green I in DMSO	0.8 µL	0.4X	6.4 µL
Nuclease-free water	11.6 µL	N/A	208.8 µL
Total volume	**20 µL**		

Table B.1B: qPCR Master Mix with no template (2 samples, 1 master mix):

Component (Template Free)	Volume	Final concentration	Master Mix volume
5X Phusion HF Buffer (5x)	4 µL	1x	12 µL
10mM dNTPs	0.4 µL	200 µM each	1.2 µL
Forward primer (10uM) RandPosA Pforward	1 µL	0.5 µM	3 µL
Reverse primer (10uM) RandPosA PReverse	1 µL	0.5 µM	3 µL
Phusion™ High–Fidelity DNA Polymerase	0.2 µL	0.02 U/µL	0.6 µL
10X SYBR Green I in DMSO	0.8 µL	0.4X	2.4 µL
Nuclease-free water	10.6 µL	N/A	31.8 µL
Total volume	**20 µL**		

B.2 – qPCR Master Mix Setup for dNTP-MNPs

Table B.2: qPCR Master Mix with template and MNPs/supernatant (3 master mixes, 21 samples):

Component	Volume	Final concentration	Master Mix volume
5X Phusion HF Buffer (5x)	4 µL	1x	32 µL
10mM dNTPs 3nuc(from separate components)	0.4 µL	200 µM each	3.2 µL
Beads or supernatant	10 µL		N/A
Forward primer (10uM) RandPosA Pforward	1 µL	0.5 µM	8 µL
Reverse primer (10uM) RandPosA PReverse	1 µL	0.5 µM	8 µL
Template DNA (RandPosA top+bottom)	1 µL	0.1-10 ng	8 µL
Phusion™ High–Fidelity DNA Polymerase	0.2 µL	0.02 U/µL	1.6 µL
10X SYBR Green I in DMSO	0.8 µL	0.4X	6.4 µL
Nuclease-free water	1.6 µL	N/A	12.8 µL
Total volume	**20 µL**		

	1	2	3	4	5	6	7	8	9	10	11	12
A	NT1					GE1	GE2	GES	GP1	GP2	GPS	NoG
B	NT2					CE1	CE2	CES	CP1	CP2	CPS	NoC
C												
D												
E												
F												
G	CNM1											
H	CNM2					TE1	TE2	TES	TP1	TP2	TPS	NoT

Figure B.1: qPCR well set up example.

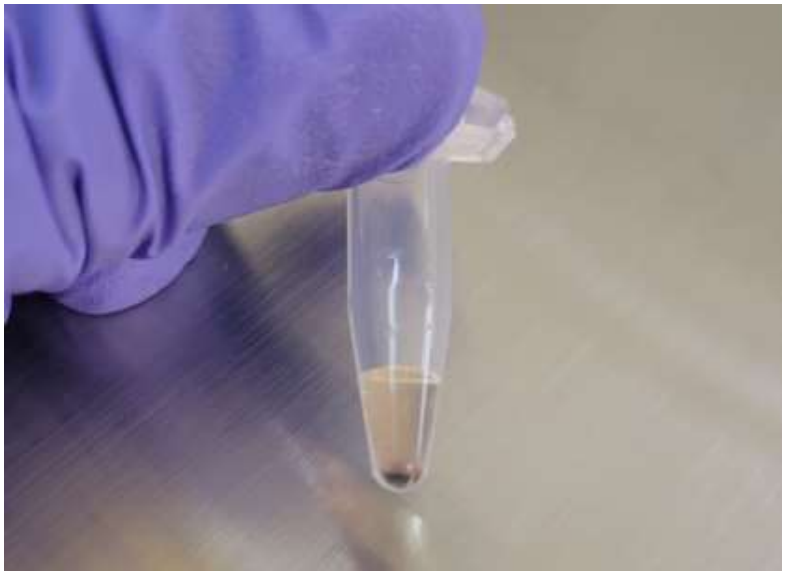

Figure B.2: dNTP-MNPs sedimenting to bottom of aqueous solution.